

Geophysical Research Letters®

RESEARCH LETTER

10.1029/2022GL099000

Key Points:

- Using Van Allen Probes data, we provide the first observational evidence for the origin of repetitive chorus emissions
- There universally exists an inverse correlation between the repetitive period of chorus emissions and drift velocity of electrons
- We propose that the day-night asymmetry of the repetitive period of chorus emissions is caused by the asymmetry of drift velocity

Correspondence to:





X. Gao and Q. Lu,
gaoxl@mail.ustc.edu.cn;
qmlu@ustc.edu.cn

Citation:

Gao, X., Chen, R., Lu, Q., Chen, L., Chen, H., & Wang, X. (2022). Observational evidence for the origin of repetitive chorus emissions. *Geophysical Research Letters*, 49, e2022GL099000. <https://doi.org/10.1029/2022GL099000>

Received 5 APR 2022
 Accepted 2 JUN 2022

Observational Evidence for the Origin of Repetitive Chorus Emissions

Xinliang Gao^{1,2,3} , Rui Chen^{1,2,3} , Quanming Lu^{1,2,3} , Lunjin Chen⁴, Huayue Chen^{1,2,3}, and Xueyi Wang⁵ 

¹CAS Key Laboratory of Geospace Environment, Department of Geophysics and Planetary Science, University of Science and Technology of China, Hefei, China, ²CAS Center for Excellence in Comparative Planetology, Hefei, China, ³Collaborative Innovation Center of Astronautical Science and Technology, Harbin, China, ⁴Department of Physics, University of Texas at Dallas, Richardson, TX, USA, ⁵Physics Department, Auburn University, Auburn, AL, USA

Abstract Chorus waves, discovered as a series of repetitive coherent emissions, are well known for producing hazard radiation environments in Earth's magnetosphere. Its repetitive nature directly causes the rapid modulation of pulsating aurora in the upper atmosphere and microburst in the ionosphere, but its origin remains a decades-old puzzle. Recent simulation suggested the energetic electrons, injected from the magnetotail and drifting eastward around the Earth, are critical to form the repetitive pattern. Based on a survey of 1.5 year data from Van Allen Probes, we provide the first observational evidence for the origin of repetitive chorus emissions. We find there exists universally an inverse correlation between the repetitive period and drift velocity of energetic electrons, uncovering how the drifting energetic electrons tune the repetitive period of chorus emissions, which is also supported by kinetic simulations. Our finding may apply to understand the generation of repetitive emissions in planetary magnetospheres and laboratory plasmas.

Plain Language Summary Whistler-mode chorus waves pervasively exist in the Earth's and other planetary outer space, which are the major contributor to hazard radiative environment near Earth and specular diffuse aurora in the upper atmosphere. They are characterized by a series of repetitive coherent emissions with the frequency chirping. Scientists have widely believed chorus waves are generated by electron injections during active periods. Although the great progress has been made on the formation of frequency chirping, the origin of its repetitive nature still challenges the community since the early space age. Here, we present a thorough analysis of 1.5 year high-resolution data from advanced NASA Van Allen Probes, and find there universally exists an inverse correlation between the repetitive period of chorus emissions and drift velocity of electrons. This result firstly uncovers how the rate of energy supplies tunes the repetitive period of chorus waves. This mechanism can also explain the well-known day-night asymmetry of the repetitive period of chorus waves. Our finding may help scientists better understand the generation of repetitive waves in an open system, such as other planetary magnetospheres and laboratory plasmas.

1. Introduction

Early space exploration beginning in the late 1960s, discovered a ubiquitous, intense electromagnetic emission at frequencies below a few kilohertz (Burtis & Helliwell, 1969; Gao et al., 2014; Li et al., 2012; Meredith et al., 2001; Tsurutani & Smith, 1974, 1977) in the near-Earth magnetized environment known as magnetosphere, as well as other planetary magnetospheres (Gurnett et al., 1981, 1986; Li et al., 2021; Scarf et al., 1979; Shprits et al., 2018). This emission is named chorus wave because it sounds like a dawn chorus of birds due to its coherent and repetitive nature (Storey, 1953). This important wave is known to efficiently accelerate electrons that are trapped in the Earth's magnetic field from energies of the order of a few keV to several MeV (Horne et al., 2005; Shprits et al., 2008; Summers et al., 1998; Thorne et al., 2013), producing the radiation hazards to satellites and human in space. Chorus wave is also responsible for the precipitation of low-energy (0.1–30 keV) electrons into the polar upper atmosphere, powering aurorae and changing high-latitude ionization and chemistry (Kasahara et al., 2018; Lam et al., 2010; Ni et al., 2008; Nishimura et al., 2010; Thorne et al., 2010).

Chorus wave typically appears as a series of periodic or quasi-periodic frequency chirpings (called elements; Burtis & Helliwell, 1969; Tsurutani & Smith, 1974; Li et al., 2012; Gao et al., 2014) in the frequency-time spectrogram. Numerous theories and simulation models have been developed to understand its generation (Kato

& Omura, 2006; Lu et al., 2019; Nunn et al., 1997; Omura et al., 2008; Tao, 2014), and the rising-tone chorus element has been successfully reproduced by relaxing a population of anisotropic electrons (i.e., perpendicular pressure larger than parallel pressure with respect to the background magnetic field). But those simulated chorus emissions have lost the repetitive nature with the presence of only one or several distinct rising-tone elements.

The repetitive nature of chorus wave exhibits not only in the rapid modulation of pulsating aurorae in the upper atmosphere (Hosokawa et al., 2020; Ozaki et al., 2019), but also in the high temporal variations (<1 s) of precipitating electron fluxes to the ionosphere (called microbursts; Lorentzen et al., 2001; Thorne et al., 2005; Tsurutani et al., 2013; Mozer et al., 2018). However, the origin of repetitive chorus emissions remains unclear for over 50 years. In the Earth's magnetosphere, chorus emissions are usually excited following the long-lasting injection of plasma sheet electrons during periods of enhanced geomagnetic activity (Li et al., 2009). Due to the inhomogeneity of Earth's inherent magnetic fields, these injected electrons drift eastward around the Earth in the magnetosphere. Lately, using a one-dimensional (1-D) δf particle-in-cell (PIC) simulation model, Lu et al. (2021) proposed that the electron injection plays an important role in forming the repetitive pattern. But no observational evidence has yet been obtained to support that.

Here we provide the first observational evidence for the origin of repetitive chorus emissions, uncovering how the drifting energetic electrons tune the repetitive period of chorus emissions. We present a survey of 1.5 year data from Van Allen Probes, showing there exists an inverse correlation between the repetitive period of chorus emissions and drift velocity of energetic electrons. Our finding can well explain the day-night asymmetry of the repetitive period of chorus emissions, that is the dayside chorus emissions typically have the longer repetitive period than nightside emissions.

2. Dataset and Simulation Model

Van Allen Probes (Mauk et al., 2013), consisting of two identical satellites (A and B), are operating in near-equatorial, highly elliptical, and low-inclination orbits with perigees of $\sim 1.1 R_E$ and apogees of $\sim 5.8 R_E$, perfectly covering the main source region (i.e., magnetic equator) of chorus emissions. The onboard Electric and Magnetic Field Instrument Suite and Integrated Science (EMFISIS) instrument (Kletzing et al., 2013) provides not only the high-resolution waveform data (35,000 samples/sec) in burst mode, but also the power spectrum data (1/6 sample/sec) in survey mode. The background magnetic field is obtained from the triaxial fluxgate magnetometer (MAG, a part of the EMFISIS instrument suite). The plasma measurement is provided by the Helium, Oxygen, Proton, and Electron (HOPE; Funsten et al., 2013) instrument.

One-dimensional (1-D) gcPIC- δf simulation model is performed in a dipole magnetic field. In this model, there are two electron components: cold and energetic electrons. All electrons are treated as particles, but ions are motionless. The simulation domain is along the magnetic field line with the magnetic latitude ranging from about -28° to 28° , and the topology of the magnetic field is roughly equal to that at $L = 0.6$. Different from previous PIC simulations, energetic electrons are continuously injected into the simulation domain in the azimuthal direction. The details about this model have been elaborated by Lu et al. (2021). In our simulations, the other parameters at the equator are initialized as follow: the ratio of number density of energetic electrons to that of cold electrons is $n_{ho}/n_{c0} = 0.6\%$, the ratio of plasma frequency to electron gyrofrequency is $\omega_{pe}/\Omega_{e0} = 5$ (where $\omega_{pe} = \sqrt{n_0 e^2 / m_e \epsilon_0}$ is the plasma frequency, $n_0 = n_{c0} + n_{ho}$, and $\Omega_{e0} = e B_{0eq} / m_e$ is the electron gyrofrequency at the equator), the temperature anisotropy of energetic electrons is $T_{\perp 0} / T_{\parallel 0} = 6$, and the parallel plasma beta of energetic electrons is $\beta_{\parallel ho} = n_{ho} T_{\parallel 0} / B_{0eq}^2 / 2 \mu_0 = 0.01$. These parameters are consistent with observations at $L = 6$ in the Earth's magnetosphere, and the other values of these parameters along the magnetic field can be obtained based on the Liouville's theorem. In each simulation, there are 4,000 grid cells, and its length is $0.34 d_e$ (where $d_e = c / \omega_{pe}$ is the electron inertial length). On average, there are about 4,000 particles in each cell, and the time step is $0.03 \Omega_{e0}^{-1}$. Absorbing boundary condition is applied for the electromagnetic field, while reflecting boundary is applied for particles.

3. Results

Chorus waves in the Earth's magnetosphere typically exhibit discrete and repetitive emissions with the rising frequency. For example, Van Allen Probe-A detected a significant enhancement of electron flux from a few keV to tens of keV on 17 March 2013 (Figure 1b), due to intense substorm injections during 22:00–23:30 UT with

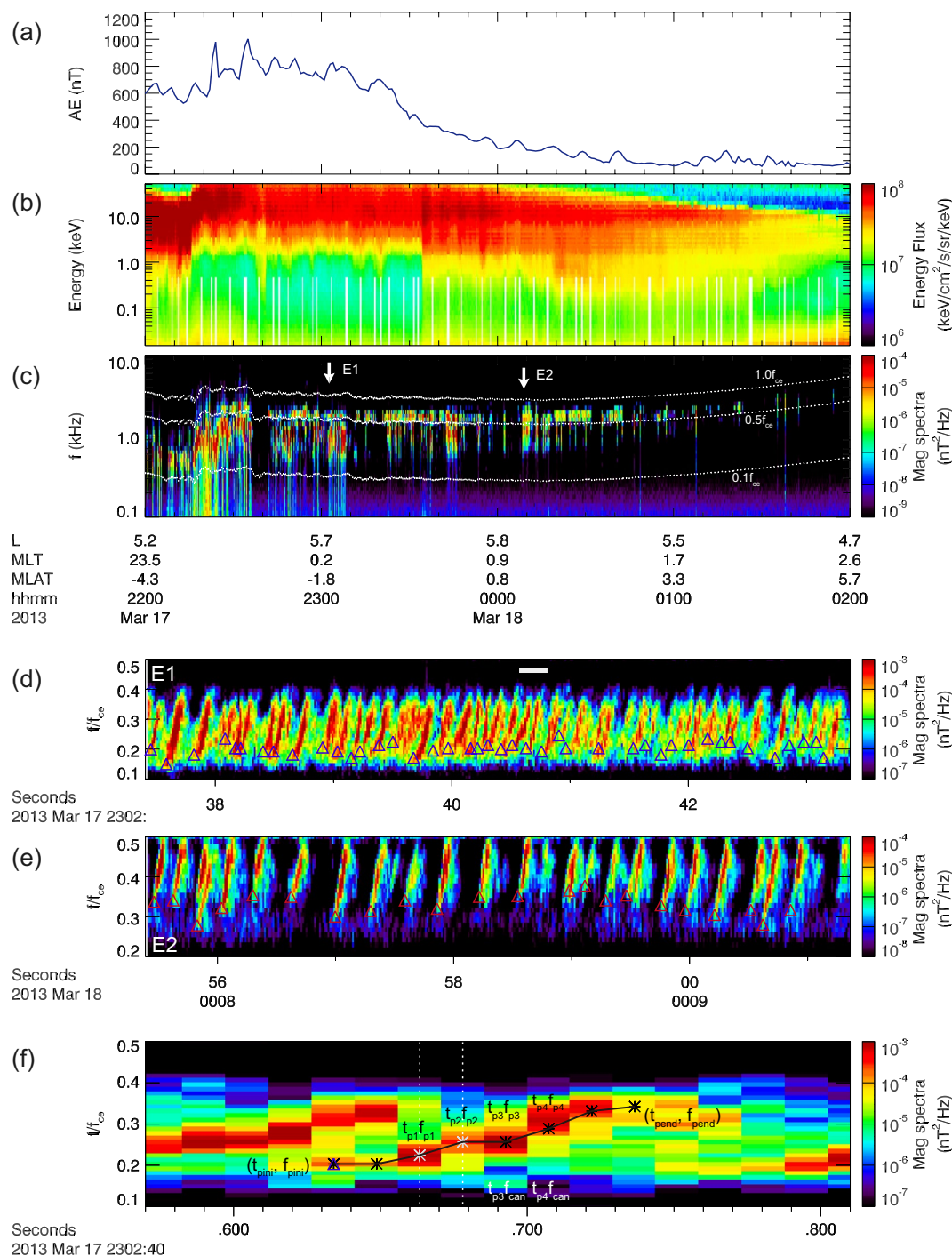


Figure 1. (a) 4 hr overview of Auroral Electrojet (AE) index, (b) electron differential energy flux measured by Van Allen Probe-A, (c) magnetic wave spectral intensity, (d and e) two 6 s high-resolution measurements of magnetic wave spectrum at E1 and E2 marked by the blue dashed lines in panel b and f enlarged view of one element marked by the white line in panel (d) Chorus waves falling in the range between $0.1 f_{ce}$ and $1.0 f_{ce}$, which are illustrated by dashed white lines.

Auroral Electrojet index larger than 500 nT (Figure 1a). Expectedly, chorus emissions were clearly observed in the frequency range between $0.1 f_{ce}$ and $1.0 f_{ce}$ (where f_{ce} is the equatorial electron gyrofrequency) during this time interval (Figure 1c), and two 6 s segments with the high-cadence magnetic field data are selected to show the zoom-in wave dynamic spectra (Figures 1d and 1e). Figure 1f presents an example (marked by the white line in Figure 1d) for illustrating how to identify the rising-tone chorus element. Firstly, we select two adjacent

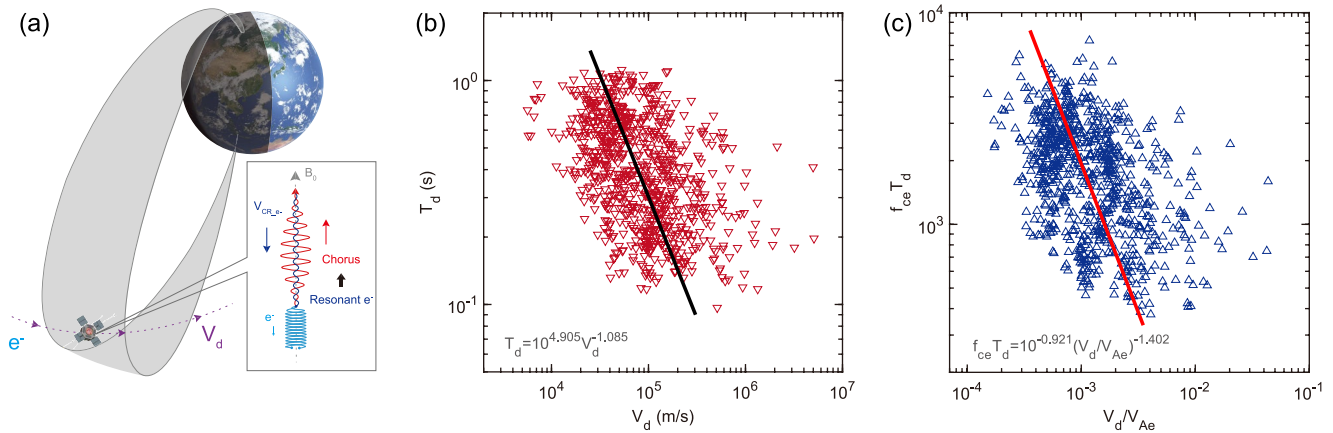


Figure 2. (a) Schematic diagrams summarizing electron drift motion (purple line), resonant electrons motion (cyan line) and chorus waves propagation (red line). Due to the gradient and curvature of background magnetic field, electrons do the eastward drift motion around the Earth. Meanwhile, resonant electrons can provide free energy for the generation of chorus waves. (b) The relation between the repetitive period T_d and drift velocity V_d of resonant energetic electrons. (c) The relation between normalized period V_d/V_{Ae} and normalized drift velocity $f_{ce} T_d$. In panel b and c, the black and red lines are the fitting curves for two distributions.

points (marked by gray stars) inside the element, that is, (t_{p1}, f_{p1}) and (t_{p2}, f_{p2}) . Here, f_{p1} (or f_{p2}) is the frequency corresponding to the maximum power over $0.1-0.5 f_{ce}$ at t_{p1} (or t_{p2}). Secondly, we use linear interpolation to get the next candidate point (t_{p3}, f_{can}) based on the two previous points. At time t_{p3} , the power-weighted average of frequency from $f_{can} - 170$ Hz to $f_{can} + 170$ Hz to obtain the next point (t_{p3}, f_{p3}) . Finally, we repeat the second step forward and backward until get the ending point (t_{pend}, f_{pend}) and initial point (t_{pini}, f_{pini}) of the element where the maximum power over $f_{can} - 170$ Hz to $f_{can} + 170$ Hz falls below one thousandth of the maximum power during the entire time interval (6 s). For an element, the frequency is further required to increase monotonically. Therefore, the extracted frequency profile of the example element is shown by the black curve. Moreover, one element is required to include at least five points, and one repetitive chorus event must include at least six rising-tone elements. The time interval Δt between two adjacent rising-tone elements is given by the time between their initial points (marked by triangles in Figures 1d and 1e). For each chorus event (6 s interval), the repetitive period T_d is obtained by averaging all Δt . Each segment, consisting of multiple nearly identical rising-tone elements, is recognized as one chorus event. In both chorus events, the rising-tone element appears one after another with an almost constant repetitive period, but repetitive periods of the two events are distinctly different, estimated as ~ 0.13 and ~ 0.26 s respectively.

Energetic electrons from Earth's magnetotail are continually injected into inner magnetosphere during substorms, and then drift eastward around the Earth caused by the inhomogeneous magnetic field (i.e., dipole field; Figure 2a). During the azimuthal drift, these energetic electrons are unstable to excite chorus waves through cyclotron resonance (Figure 2a). Van Allen Probes can be treated as stationary during such a short time interval (i.e., 6 s), since the satellite velocity (1–10 km/s) is far less than the drift velocity of energetic electrons (~ 570 km/s at energy ~ 34.2 keV). As these electrons pass by the same field line where the satellite locates, the rising-tone chorus element will be triggered one after another due to the continuous supplies of free energy in electrons and then propagate toward the satellite. Therefore, it is natural to speculate the repetitive period T_d of chorus emissions should be controlled by the rate of energy supplies, that is, the drift velocity V_d of energetic electrons.

Since chorus waves are generated by energetic electrons through cyclotron resonance, so we need to estimate the drift velocity V_d of resonant electrons. The parallel velocity $v_{\parallel r}$ of resonant electrons is determined by the first-order cyclotron resonance condition

$$\omega - k_{\parallel} v_{\parallel r} = \Omega_{ce}, \quad (1)$$

where ω is wave angular frequency, and k_{\parallel} is the parallel component (relative to background magnetic field) of wave number. Here, the ω is given by $2\pi f_{pini}$, since previous theories and simulations suggested that rising-tone chorus element is triggered by the triggering wave (i.e., at the initial wave frequency f_{pini} ; Katoh & Omura, 2006; Hikishima & Omura, 2012). The wave number is estimated based on the cold plasma dispersion relation

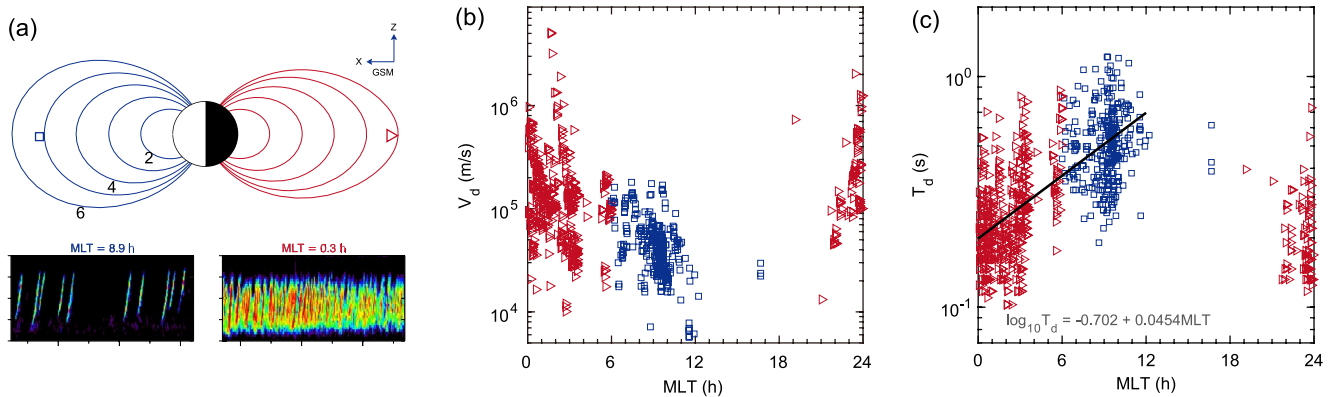


Figure 3. (a) The day-night asymmetric configuration of magnetic field under the strong solar wind environment. At the bottom, the magnetic spectrums of two 6 s rising-tone chorus events are presented, where the left one is captured at dayside (i.e., MLT = 8.9 hr) and the right one is captured at night side (i.e., MLT = 0.3 hr), while both events are at close L -shell and magnetic latitude. (b) The distribution between drift velocity V_d and MLT. (c) The distribution between repetitive period T_d and MLT. In panels b and c, the event at nightside (MLT, 0–6, 18–24 hr) is marked by red triangle, and the event at dayside (MLT, 6–18 hr) is marked by blue square. The black line is the fitting curve for the repetitive period between 0 and 12 hr in panel (c).

(Stix, 1962). Since the drift velocity of resonant electrons is caused by the curvature and gradient of the Earth's magnetic field, then the drift velocity can be estimated by the formula

$$\vec{V}_d = \frac{2E_{\parallel} + E_{\perp}}{qB_0^3} \vec{B}_0 \times \nabla \vec{B}_0, \quad (2)$$

where $E_{\parallel} = \frac{1}{2}mv_{\parallel}^2$ is the parallel kinetic energy of resonant electrons, and E_{\perp} is the perpendicular kinetic energy. For simplicity, we assume E_{\perp} to be three times E_{\parallel} , meaning the pitch angle of electrons is 60° . Other pitch angles are also tested, and the principal results remain unchanged. $\nabla \vec{B}_0$ can be calculated from the magnetic field model, such as Ts04 model (Tsyganenko & Sitnov, 2005). After the drift velocity for each rising-tone element is obtained, then we average all of them to get the V_d for this event. For example, the drift velocities V_d for event E1 and E2 are ~ 570 km/s and ~ 100 km/s, respectively.

To determine the correlation between repetitive period T_d and drift velocity V_d , we have collected chorus events (793 in total) detected by Van Allen Probe-A from January 2013 to August 2014, and extracted the values of T_d and V_d for each event. As shown in Figure 2b, there is a clear inverse correlation between repetitive period T_d and drift velocity V_d , which can be approximately described as $T_d = 10^{4.905} V_d^{-1.085}$ through the least square fitting. This result suggests energetic electrons with a larger V_d , the faster energy injection, will produce chorus elements of shorter separations. Considering the background plasma condition for each event is quite different in Earth's magnetosphere, we also normalize the V_d and T_d by the local electron Alfvén velocity (V_{Ae}) and gyrofrequency (f_{ce}). Figure 2c shows a similar inverse correlation between them, approximately described as $f_{ce} T_d = 10^{-0.921} (V_d / V_{Ae})^{-1.402}$.

Solar wind, a stream of plasma released from the upper atmosphere of the sun, reshapes the Earth's magnetosphere as shown in Figure 3a, where the dayside field line becomes compressed, while the nightside field line becomes more stretched (Figure 3a). This permanent asymmetric inhomogeneity of magnetic fields naturally leads to the day-night asymmetry of the drift velocity of energetic electrons (Figure 3b). Since the repetitive period of chorus emission is controlled by the drift velocity, then it is easily to conclude that the repetitive period of chorus emission should also exhibit the day-night asymmetry. Taking two chorus events as examples, we can clearly find the chorus event at magnetic local time (MLT) = 8.9 hr has a much longer repetitive period than the one at MLT = 0.3 hr (Figure 3a). The distribution of repetitive periods of all chorus events in Figure 2a over MLT is illustrated in Figure 3c, which shows a distinct day-night asymmetry. Specifically, the repetitive period tends to increase from midnight (MLT = 0 or 24 hr) toward noon (MLT = 12 hr). The repetitive period of chorus waves at nightside ranges from ~ 0.1 to ~ 0.4 s, while at dayside the repetitive period falls between ~ 0.3 and ~ 0.9 s. This statistical result reveals that the geometry of Earth's magnetic field plays an important role in determining the repetitive period of chorus emissions.

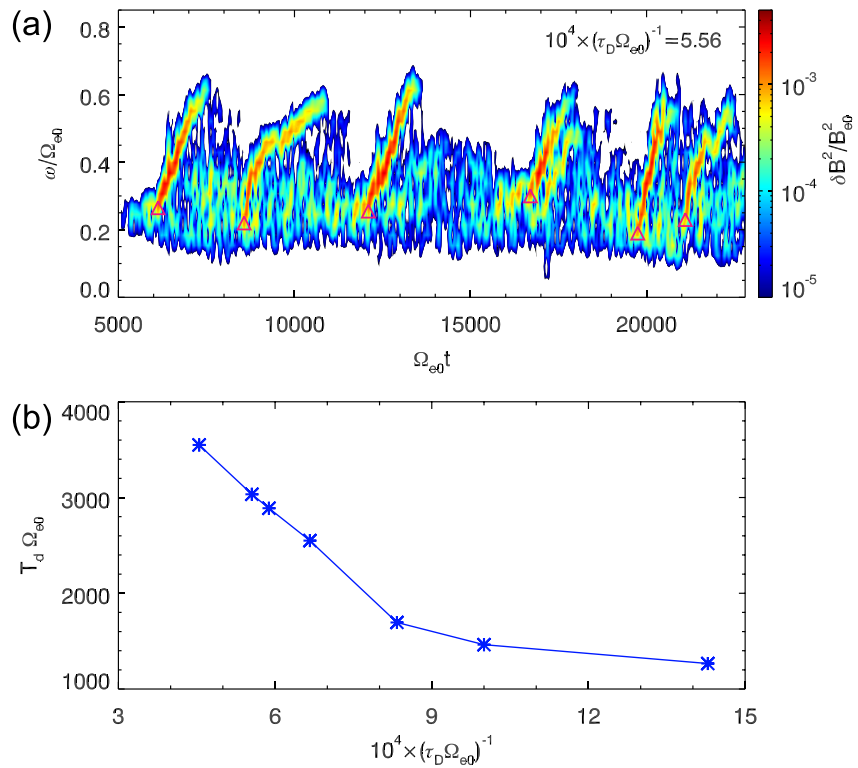


Figure 4. (a) The fluctuating magnetic spectrum of $\delta B^2/B_{e0}^2$ ($\delta B^2 = \delta B_x^2 + \delta B_y^2 + \delta B_z^2$) in the case with $\tau_D \Omega_{e0} = 1,800$, where the starting point of each rising tone element is denoted by magenta triangle. (b) The T_d as a function of τ_D , in which the simulation cases are represented by blue asterisks, with a blue line connecting them.

Using the same one-dimensional (1-d) δf simulation model as Lu et al. (2021), we have further studied the correlation between the repetitive period of rising-tone chorus emissions and drift velocity of anisotropic electrons. In this model, anisotropic electrons are continuously injected into the simulation system with a constant drift velocity that can be expressed by τ_D^{-1} . The smaller τ_D represents the larger drift velocity of injection. Figure 4a shows the simulated chorus emissions for the case with $\tau_D \Omega_{e0} = 1,800$, where six clear rising-tone elements can be observed. This repetitive chorus emission is quite similar to that observed in the magnetosphere (Figures 1d and 1e). The repetitive period is estimated as $\sim 3,034 \Omega_{e0}^{-1}$ for this case. We have simulated 7 cases with different values of τ_D , that is, 700, 1,000, 1,200, 1,500, 1,700, 1,800, and 2,200 Ω_{e0}^{-1} . For each case, the repetitive rising-tone chorus is excited and its repetitive period is extracted using the same method applied for observed chorus waves. As shown in Figure 4b, we can also find that there exists an inverse correlation between T_d and τ_D^{-1} , which qualitatively agrees with the statistical result presented in Figures 2b and 2c. However, it still remains computationally challenging to quantitatively compare simulations with observations, because such kinetic simulations using the realistic parameters require extremely huge computing resource.

4. Conclusion and Discussion

Chorus wave typically appears as a series of periodic or quasi-periodic frequency chirpings, and its repetitive nature can directly lead to the rapid modulation of pulsating aurorae in the upper atmosphere (Hosokawa et al., 2020; Ozaki et al., 2019) and the microbursts in the ionosphere (Lorentzen et al., 2001; Mozer et al., 2018; Thorne et al., 2005; Tsurutani et al., 2013). In this report, we provide the first direct observational evidence for the origin of repetitive chorus emissions, uncovering how the drift velocity of injections controls the repetitive period of chorus emissions. Based on 1.5 year high-resolution Van Allen Probes data, combining with the Ts04 magnetic field model, we find there exists an inverse correlation between the repetitive period of chorus emissions and drift velocity of energetic electrons. The faster drift typically produces more frequent chorus elements, consistent with the 1-D δf simulation results. Our study can well explain the day-night asymmetry of the repetitive

period of chorus emissions, that is the dayside chorus emissions typically have the longer repetitive period than nightside emissions.

When the free energy of energetic electrons is sufficiently large, a nonlinear wave growth leads to an increasing amplitude. Accompanied with it, the frequency increases and thus a rising-tone chorus element is formed. During the chorus element formation, the free energy is rapidly released due to the scattering by the formed chorus element. The refilling due to the electron injection starts to restore the free energy, and when the free energy exceeds the threshold of nonlinear wave growth, another cycle of chorus element formation starts. Therefore, the period of the repetitive cycle depends on the refilling rate, which explains the dependence of the repetitive period of chorus elements on the refilling rate (i.e., the drift velocity).

The Sun is the ultimate source of energy to power all dynamics in the Earth's outer space, but the underlying physical principals still remains one of the most challenging problems. The solar wind permanently compresses the Earth's dipole magnetic field at dayside, and drags the magnetic field at nightside (Tsyganenko & Sitnov, 2005). Due to the asymmetric background magnetic field, the drift velocity of energetic electrons injected from the magnetotail will decrease during the eastward drift (i.e., from midnight to noon; Figure 3b). In this report, we find there is a clear trend that the repetitive period of chorus emissions increases from midnight to noon (Figure 3c), which is caused by the asymmetric drift velocity of energetic electrons over MLT. Our study presents a potential way of how the macroscopic solar wind affects the microscopic wave-particle interactions inside the Earth's magnetosphere.

Repetitive chorus emissions are observed not only in the Earth's magnetosphere (Burtis & Helliwell, 1969; Gao et al., 2014; Li et al., 2012; Meredith et al., 2001; Tsurutani & Smith, 1974), but also in other planetary magnetospheres (Gurnett et al., 1981, 1986; Li et al., 2021; Scarf et al., 1979) and laboratory plasma device (Van Compernelle et al., 2015). Therefore, the repetitive pattern could be a common character for chorus emissions generated in an open system, where the electron free energy continuously supplies. The drift velocity of energetic electrons, how fast the free energy supplies, should be the key factor to tune the repetition of chorus emission in such system. This drift-driving mechanism, supported by observations and simulations, may also apply to the generation of repetitive emissions in other open systems.

Data Availability Statement

The entire Van Allen Probes data set is publicly available at <https://spdf.gsfc.nasa.gov/pub/data/rbsp/>. The input parameters for Ts04 magnetic model are available at http://geo.phys.spbu.ru/~tsyganenko/TS05_data_and_stuff/. The Van Allen Probe data analysis is carried out using the publicly available Space Physics Environment Data Analysis Software (SPEDAS, <http://spedas.org>). The computer code of δf simulation in this work is available upon request to the corresponding author. The simulation data can be accessed via <https://dx.doi.org/10.12176/01.99.01876>.

References

- Burtis, W. J., & Helliwell, R. A. (1969). Banded chorus-A new type of VLF radiation observed in the magnetosphere by OGO 1 and OGO 3. *Journal of Geophysical Research*, *74*(11), 3002–3010. <https://doi.org/10.1029/ja074i011p03002>
- Funsten, H. O., Skoug, R. M., Guthrie, A. A., MacDonald, E. A., Baldonado, J. R., Harper, R. W., et al. (2013). Helium, oxygen, proton, and electron (HOPE) mass spectrometer for the Radiation Belt Storm Probes mission. *Space Science Reviews*, *179*, 423–484. <https://doi.org/10.1007/s11214-013-9968-7>
- Gao, X., Li, W., Thorne, R. M., Bortnik, J., Angelopoulos, V., Lu, Q., et al. (2014). New evidence for generation mechanisms of discrete and hiss-like whistler mode waves. *Geophysical Research Letters*, *41*, 4805–4811. <https://doi.org/10.1002/2014gl060707>
- Gurnett, D. A., Kurth, W. S., & Scarf, F. L. (1981). Plasma waves near Saturn: Initial results from Voyager 1. *Science*, *212*, 235–239. <https://doi.org/10.1126/science.212.4491.235>
- Gurnett, D. A., Kurth, W. S., Scarf, F. L., & Poynter, R. L. (1986). First plasma wave observations at Uranus. *Science*, *233*, 106–109. <https://doi.org/10.1126/science.233.4759.106>
- Hikishima, M., & Omura, Y. (2012). Particle simulations of whistler-mode rising-tone emissions triggered by waves with different amplitudes. *Journal of Geophysical Research*, *117*, A04226. <https://doi.org/10.1029/2011JA017428>
- Horne, R. B., Thorne, R. M., Glauert, S. A., Albert, J. M., Meredith, N. P., & Anderson, R. R. (2005). Timescale for radiation belt electron acceleration by whistler mode chorus waves. *Journal of Geophysical Research*, *110*, A03225. <https://doi.org/10.1029/2004JA010811>
- Hosokawa, K., Miyoshi, Y., Ozaki, M., Oyama, S. I., Ogawa, Y., Kurita, S., et al. (2020). Multiple time-scale beats in aurora: Precise orchestration via magnetospheric chorus waves. *Scientific Reports*, *10*, 3380. <https://doi.org/10.1038/s41598-020-59642-8>
- Kasahara, S., Miyoshi, Y., Yokota, S., Mitani, T., Kasahara, Y., Matsuda, S., et al. (2018). Pulsating aurora from electron scattering by chorus waves. *Nature*, *554*(7692), 337–340. <https://doi.org/10.1038/nature25505>

Acknowledgments

This research was funded by the Strategic Priority Research Program of Chinese Academy of Sciences Grant No. XDB41000000, Key Research Program of Frontier Sciences CAS (QYZDJ-SSW-DQC010), the Fundamental Research Funds for the Central Universities (WK3420000013), and “USTC Tang Scholar” program. We acknowledge the entire Van Allen Probes instrument teams. We also acknowledge for the data resource from “National Space Science Data Center, National Science & Technology Infrastructure of China (<http://www.nssc.ac.cn>).

- Katoh, Y., & Omura, Y. (2006). A study of generation mechanism of VLF triggered emission by self-consistent particle code. *Journal of Geophysical Research*, *111*, A12207. <https://doi.org/10.1029/2006JA011704>
- Kletzing, C. A., Kurth, W. S., Acuna, M., MacDowall, R. J., Torbert, R. B., Averkamp, T., et al. (2013). The electric and magnetic field instrument suite and integrated science (EMFISIS) on RBSP. *Space Science Reviews*, *179*(1–4), 127–181. <https://doi.org/10.1007/s11214-013-9993-6>
- Lam, M. M., Horne, R. B., Meredith, N. P., Glauert, S. A., Moffat-Griffin, T., & Green, J. C. (2010). Origin of energetic electron precipitation >30 keV into the atmosphere. *Journal of Geophysical Research*, *115*, A00F08. <https://doi.org/10.1029/2009JA014619>
- Li, W., Ma, Q., Shen, X.-C., Zhang, X.-J., Mauk, B. H., Clark, G., et al. (2021). Quantification of diffuse auroral electron precipitation driven by whistler mode waves at Jupiter. *Geophysical Research Letters*, *48*, e2021GL095457. <https://doi.org/10.1029/2021GL095457>
- Li, W., Thorne, R. M., Angelopoulos, V., Bonnell, J. W., McFadden, J. P., Carlson, C. W., et al. (2009). Evaluation of whistler-mode chorus intensification on the nightside during an injection event observed on the THEMIS spacecraft. *Journal of Geophysical Research*, *114*, A00C14. <https://doi.org/10.1029/2008JA013554>
- Li, W., Thorne, R. M., Bortnik, J., Tao, X., & Angelopoulos, V. (2012). Characteristics of hiss-like and discrete whistler mode emissions. *Geophysical Research Letters*, *39*, L18106. <https://doi.org/10.1029/2012GL053206>
- Lorentzen, K. R., Blake, J. B., Inan, U. S., & Bortnik, J. (2001). Observations of relativistic electron microbursts in association with VLF chorus. *Journal of Geophysical Research*, *106*(A4), 6017–6027. <https://doi.org/10.1029/2000JA003018>
- Lu, Q., Chen, L., Wang, X., Gao, X., Lin, Y., & Wang, S. (2021). Repetitive emissions of rising-tone chorus waves in the inner magnetosphere. *Geophysical Research Letters*, *48*, e2021GL094979. <https://doi.org/10.1029/2021GL094979>
- Lu, Q., Ke, Y., Wang, X., Liu, K., Gao, X., Chen, L., & Wang, S. (2019). Two-dimensional general curvilinear particle-in-cell (gcPIC) simulation of rising-tone chorus waves in a dipole magnetic field. *Journal of Geophysical Research: Space Physics*, *124*, 4157–4167. <https://doi.org/10.1029/2019JA026586>
- Mauk, B. H., Fox, N. J., Kanekal, S. G., Kessel, R. L., Sibeck, D. G., & Ukhorskiy, A. (2013). Science objectives and rationale for the radiation belt storm Probes mission. *Space Science Reviews*, *179*, 3–27. <https://doi.org/10.1007/s11214-012-9908-y>
- Meredith, N. P., Horne, R. B., & Anderson, R. R. (2001). Substorm dependence of chorus amplitudes: Implications for the acceleration of electrons to relativistic energies. *Journal of Geophysical Research*, *106*(A7), 13165–13178. <https://doi.org/10.1029/2000JA900156>
- Mozer, F. S., Agapitov, O. V., Blake, J. B., & Vasko, I. Y. (2018). Simultaneous observations of lower band chorus emissions at the equator and microburst precipitating electrons in the ionosphere. *Geophysical Research Letters*, *45*, 511–516. <https://doi.org/10.1002/2017GL076120>
- Ni, B., Thorne, R. M., Shprits, Y. Y., & Bortnik, J. (2008). Resonant scattering of plasma sheet electrons by whistler-mode chorus: Contribution to diffuse auroral precipitation. *Geophysical Research Letters*, *35*, L11106. <https://doi.org/10.1029/2008GL034032>
- Nishimura, Y., Bortnik, J., Li, W., Thorne, R. M., Lyons, L. R., Angelopoulos, V., et al. (2010). Identifying the driver of pulsating aurora. *Science*, *330*(6000), 81–84. <https://doi.org/10.1126/science.1193186>
- Nunn, D., Omura, Y., Matsumoto, H., Nagano, I., & Yagitani, S. (1997). The numerical simulation of VLF chorus and discrete emissions observed on the Geotail satellite using a Vlasov code. *Journal of Geophysical Research*, *102*(A12), 27083–27097. <https://doi.org/10.1029/97JA02518>
- Omura, Y., Katoh, Y., & Summers, D. (2008). Theory and simulation of the generation of whistler-mode chorus. *Journal of Geophysical Research*, *113*, A04223. <https://doi.org/10.1029/2007JA012622>
- Ozaki, M., Miyoshi, Y., Shiokawa, K., Hosokawa, K., Oyama, S. I., Kataoka, R., et al. (2019). Visualization of rapid electron precipitation via chorus element wave-particle interactions. *Nature Communications*, *10*, 257. <https://doi.org/10.1038/s41467-018-07996-z>
- Scarf, F. L., Gurnett, D. A., & Kurth, W. S. (1979). Jupiter plasma wave observations: An initial voyager 1 overview. *Science*, *204*(4396), 991–995. <https://doi.org/10.1126/science.204.4396.991>
- Shprits, Y. Y., Menietti, J. D., Drozdov, A. Y., Horne, R. B., Woodfield, E. E., Groene, J. B., et al. (2018). Strong whistler mode waves observed in the vicinity of Jupiter's moons. *Nature Communications*, *9*, 3131. <https://doi.org/10.1038/s41467-018-05431-x>
- Shprits, Y. Y., Subbotin, D. A., Meredith, N. P., & Elkington, S. R. (2008). Review of modeling of losses and sources of relativistic electrons in the outer radiation belt II: Local acceleration and loss. *Journal of Atmospheric and Solar-Terrestrial Physics*, *70*, 1694–1713. <https://doi.org/10.1016/j.jastp.2008.06.008>
- Stix, T. H. (1962). *The theory of plasma waves*. McGraw-Hill.
- Storey, L. R. O. (1953). An investigation of whistling atmospherics. *Philosophical Transactions of the Royal Society of London*, *246*, 113. <https://doi.org/10.1098/rsta.1953.0011>
- Summers, D., Thorne, R. M., & Xiao, F. L. (1998). Relativistic theory of wave-particle resonant diffusion with application to electron acceleration in the magnetosphere. *Journal of Geophysical Research*, *103*(A9), 20487–20500. <https://doi.org/10.1029/98JA01740>
- Tao, X. (2014). A numerical study of chorus generation and the related variation of wave intensity using the DAWN code. *Journal of Geophysical Research: Space Physics*, *119*, 3362–3372. <https://doi.org/10.1002/2014JA019820>
- Thorne, R. M., Li, W., Ni, B., Ma, Q., Bortnik, J., Chen, L., et al. (2013). Rapid local acceleration of relativistic radiation-belt electrons by magnetospheric chorus. *Nature*, *504*, 411–414. <https://doi.org/10.1038/nature12889>
- Thorne, R. M., Ni, B., Tao, X., Horne, R. B., & Meredith, N. P. (2010). Scattering by chorus wave as the dominant cause of diffuse auroral precipitation. *Nature*, *467*, 934–936. <https://doi.org/10.1038/nature09467>
- Thorne, R. M., O'Brien, T. P., Shprits, Y. Y., Summers, D., & Horne, R. B. (2005). Timescale for MeV electron microburst loss during geomagnetic storms. *Journal of Geophysical Research*, *110*, A09202. <https://doi.org/10.1029/2004JA010882>
- Tsurutani, B. T., Lakhina, G. S., & Verkhoglyadova, O. P. (2013). Energetic electron (>10 keV) microburst precipitation, similar to 5–15 s X-ray pulsations, chorus, and wave-particle interactions: A review. *Journal of Geophysical Research: Space Physics*, *118*, 2296–2312. <https://doi.org/10.1002/jgra.50264>
- Tsurutani, B. T., & Smith, E. J. (1974). Postmidnight chorus: A substorm phenomenon. *Journal of Geophysical Research*, *79*, 118–127. <https://doi.org/10.1029/Ja079i001p00118>
- Tsurutani, B. T., & Smith, E. J. (1977). Two types of magnetospheric ELF chorus and their substorm dependences. *Journal of Geophysical Research*, *82*(32), 5112–5128. <https://doi.org/10.1029/JA082i032p05112>
- Tsyganenko, N. A., & Sitnov, M. I. (2005). Modeling the dynamics of the inner magnetosphere during strong geomagnetic storms. *Journal of Geophysical Research*, *110*, A03208. <https://doi.org/10.1029/2004JA010798>
- Van Compernelle, B., An, X., Bortnik, J., Thorne, R. M., Pribyl, P., & Gekelman, W. (2015). Excitation of chirping whistler waves in a laboratory plasma. *Physical Review Letters*, *114*(24), 245002. <https://doi.org/10.1103/physrevlett.114.245002>